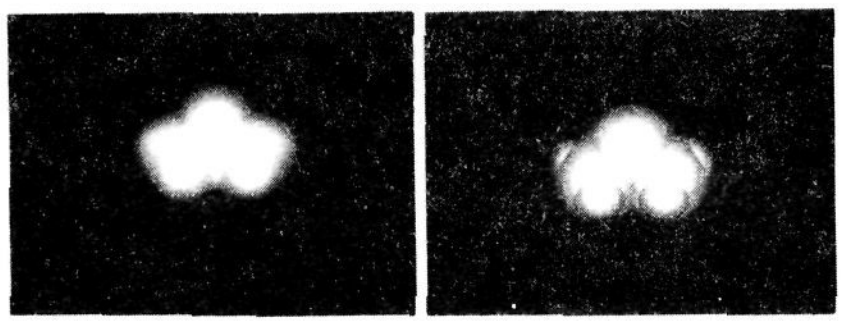

Figure 1. Left: total electron density of CH_3SCH_3. HF/3-21G(*)//HF/3-21G(*). Right: best fit by nuclear-centered spheres of total electron density.

in the original paper.[8] The image on the right-hand side of Figure 1 represents the least-squares fit to the total electron density surface by a set of spheres centered at the individual atomic positions. Visual inspection reveals that, aside from the "seams" in the sphere-fit-model, the two images are nearly identical. This is also the case for the remainder of the systems examined in this paper. Best atomic radii, r, are established by the following iterative procedure, starting from an arbitrary initial guess and continuing until self-consistent. For each atom in a molecule: (a) select from a set of 194 points spaced (approximately) uniformly on the surface of a sphere of radius r[9] those points that *do not* fall inside spheres associated with other atoms; (b) for each such point, calculate the gradient of the total electron density and move along the gradient direction until contacting the actual density surface of the molecule, i.e., $\psi^2 = 0.002$; (c) obtain a new radius as the average distance from the center of the sphere to each of the contact points.

Calculated sizes for sulfur in a variety of its simple compounds are given in Table I. Size data for the free atom in its ^3P ground state, as well as for S^+ (^4S) and S^- (^2P), are also provided and correlate linearly with atomic charge. Calculated sizes for sulfur in molecules, brought onto the same scale, lead then to specification of formal charge in these systems. These are also given in Table I and are compared to atomic charges obtained from a standard Mulliken population analysis.[10,11] The following points are worthy of comments:

1. Calculated atom sizes in the inorganic sulfur compounds (except SCl_2) closely parallel formal oxidation numbers.[12] For example, the sulfur atom in SO_3 (formally S^{VI}) is 0.08 and 0.09 Å smaller than those in SF_4 and SO_2, respectively (both formally S^{IV}). The sulfurs in these two molecules are 0.07 and 0.06 Å smaller than that in SF_2 (S^{II}), which, in turn, is 0.07 Å smaller than the value for the free atom (S^0). The calculated size of sulfur in sulfur dichloride is similar to that in the free atom, suggesting assignment of oxidation state as S^0 rather than as S^{II} (as in SF_2). Formal oxidation states for sulfur bonded to carbon are more difficult to assign (the two elements have about the same electronegativity), and correlations here are less meaningful.

2. Atomic charges based on atom sizes only roughly parallel those obtained from a Mulliken population analysis. According to both schemes, sulfur is positively charged in hypervalent compounds and (nearly) neutral or negatively charged in normal-valent systems. Mulliken charges for all compounds are more positive than those obtained by size correlations. In addition some specific and significant differences do exist between the two sets of "charges". For example, Mulliken charges for what apear to be two closely related molecules, CH_3CH_2SH and CH_3SCH_3, differ greatly, while those based on size are identical, i.e., the calculated size of the sulfur in each of these compounds is the same.

Further efforts are underway to establish the sizes of atoms (and common groups of atoms) in a variety of molecular environments and to explore additional correlations between atom size in molecules and observable properties.

Table I. Calculated Sizes and Atomic Charges for Sulfur in Molecules[a]

molecule	calcd radius, Å	charge on S (×10^{-2} electrons): from fit to total electron density	charge on S (×10^{-2} electrons): from Mulliken population analysis
SO_3	1.76	134	145
S^+	1.81	100	100
SF_4	1.84	82	163
SO_2	1.85	70	100
SF_2	1.91	40	77
S	1.96	0	0
CS_2	1.98	−10	10
SCl_2	1.99	−16	26
SCO	2.00	−27	2
CH_2CH_2S	2.00	−28	7
H_2S	2.01	−33	−27
H_2S_2	2.02	−36	−14
$S(CH_3)_2$	2.03	−45	17
CH_3CH_2SH	2.03	−45	−5
S^-	2.11	−100	−100

[a] HF/3-21G(*)//HF/3-21G(*) level. Optimum structures from ref 3, except the following: SF_2, C_{2v}, r(SF) = 1.592, ∠FSF = 98.3; CS_2, $D_{\infty h}$, r(CS) = 1.542; SCl_2, C_{2v}, r(SCl) = 2.019, ∠ClSCl = 102.5; SCO, $C_{\infty v}$, r(CS) = 1.565, r(CO) = 1.147; CH_2CH_2S, C_{2v}, r(CC) = 1.490, r(CS) = 1.817, r(CH) = 1.071, ∠HH′CC = 150.8, ∠HCH = 115.3, $S(CH_3)_2$, C_{2v}, r(CS) = 1.813, $r(CH_t)$ = 1.082, $r(CH_g)$ = 1.082, ∠CSC = 99.4, $\angle H_tCS$ = 107.7, $\angle H_{gg'}CS$ = 128.2, $\angle H_gCH_g'$ = 109.6; CH_3CH_2SH, C_s, r(CC) = 1.541, r(CS) = 1.829, $r(C_1H_t)$ = 1.084, $r(C_1H_g)$ = 1.083, $r(C_2H_g)$ = 1.081, r(SH) = 1.327, ∠CCS = 109.1, $\angle H_tC_1C_2$ = 109.9, $\angle H_{gg'}C_1C_2$ = 127.2, $\angle H_gC_1H_g'$ = 108.6, $\angle H_{gg'}C_2C_1$ = 126.1, $\angle H_gC_2H_g'$ = 108.9, ∠CSH = 97.9.

(8) (a) R. F. Hout, Jr., W. J. Pietro, and W. J. Hehre, *J. Comput. Chem.*, in press; see also (b) R. F. Hout, Jr., W. J. Pietro, and W. J. Hehre, "A Pictorial Approach to Molecular Structure and Reactivity", Wiley, New York, in press.

(9) Larger uniform sampling arrays have been found to yield optimum atomic radii to within 0.005 Å of the values reported here.

(10) R. S. Mulliken, *J. Chem. Phys.*, **23**, 1833, 1841, 2338, 2343 (1955).

(11) Among the alternative approaches to defining the charges on atoms in molecules are those due to Streitwieser (D. L. Grier and A. Streitwieser, Jr., *J. Am. Chem. Soc.*, **104**, 3556 (1982), and references therein) and to Bader (R. F. W. Bader and T. T. Nguyen-Dang, *Adv. Quantum Chem.*, **14**, 63 (1981), and references therein).

(12) For a recent discussion of other attempts to relate electron densities to formal oxidation numbers, see: K. Takano, H. Hosoya, and S. Iwata, *J. Am. Chem. Soc.*, **104**, 3998 (1982), and references therein.

Direct Observation of Radical-Pair Interaction and Decay in Anionic Micelles. A Time-Resolved Electron-Spin-Echo Study†

M. C. Thurnauer* and D. Meisel

Chemistry Division, Argonne National Laboratory Argonne, Illinois 60439

Received January 19, 1983

Photochemical reactions in micelles currently receive considerable attention.[1-5] They provide models for reactions in biological

† Work performed under the auspices of the Office of Basic Energy Sciences, Division of Chemical Sciences, U.S. Department of Energy, under Contract W-31-109-ENG-38.

(1) (a) Turro, N. J.; Krauetler, B. *J. Am. Chem. Soc.* **1978**, *100*, 7431. (b) Turro, N. J.; Kraeutler, B.; Anderson, D. R. *Ibid.* **1979**, *101*, 7435. (c) Turro, N. J., Grätzel, M.; Braun, A. M. *Angew. Chem., Int. Ed. Engl.* **1980**, *19*, 675. (d) Turro, N. J.; Chung, C.-J.; Jones, G., II; Becker W. G. *J. Phys. Chem.* **1982**, *86*, 3677.

(2) Thomas, J. K. *Chem. Rev.* **1980**, *80*, 283.

(3) Scaiano, J. C.; Abuin, E. B. *Chem. Phys. Lett.* **1981**, *81*, 209. (b) Scaiano, J. C.; Abuin, E. B.; Stewart, L. C. *J. Am. Chem. Soc.* **1982**, *104*, 5613.

(4) (a) Sakaguchi, Y.; Nagakura, S.; Hayaski, H. *Chem. Phys. Lett.* **1980**, *72*, 420. (b) Hayashi, H.; Sakaguchi, Y.; Nagakura, S. *Chem. Lett.* **1980**, 1149. (c) Sakaguchi, Y.; Nagakura, S.; Minoh, A.; Hayashi, H. *Chem. Phys. Lett.* **1981**, *82*, 213. (d) Sakaguchi, Y.; Hayashi, H. *Ibid.* **1982**, *87*, 539. (e) Sakaguchi, Y.; Hayashi, H.; Nagakura, S. *J. Phys. Chem.* **1982**, *86*, 3177.

0002-7863/83/1505-3729$01.50/0

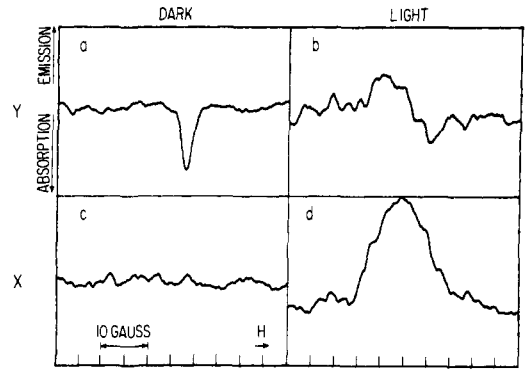

Figure 1. EPR spectra (echo intensity as a function of magnetic field) taken within 40 ns of laser excitation of 1.6×10^{-3} M benzophenone and 0.032 M 1,4-cyclohexadiene in 0.22 M SDS (τ = 620 ns): (a) Y signal dark; (b) Y signal light − dark; (c) X signal dark; (d) X signal light, $\Delta H \cong 14$ G, $g = 2.0029$.

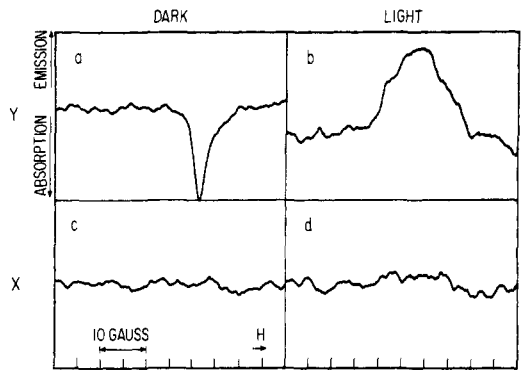

Figure 2. EPR spectra (echo intensity as a function of magnetic field) taken within 40 ns of laser excitation of 1 M benzophenone and 1.5 M 1,4-cyclohexadiene in benzene (τ = 620 ns): (a) Y signal dark; (b) Y signal light − dark, $\Delta H \cong 14$G, $g = 2.0030$; (c) X signal dark; (d) X signal light.

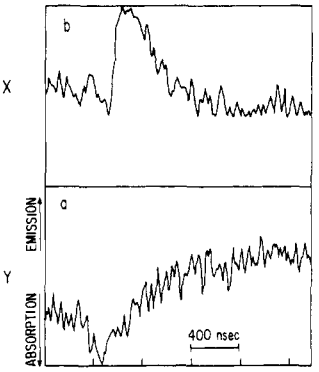

Figure 3. Kinetic traces (echo intensity as a function of time with respect to laser pulse): (a) Y signal, τ = 520 nsec. Note the initial absorption "spike" may be due to laser artifacts or slight offset of magnetic field to high-field side (Figure 1b) where at very early times the radical pair shows absorption. (b) X signal. Field set at maximum intensity Figure 1d; τ = 520 ns.

membranes and are also relevant to photochemical energy conversion problems. Recently attention has been drawn to the influence of micelles on radical-pair interactions that can, in turn, control reaction selectivity.[1,3,4] This results from the competition between intersystem crossing within the radical pair and radical escape from the micelle. The former controls the probability of chemical reaction (e.g., recombination) and can be influenced by the application of a magnetic field. Therefore, it is important to understand the magnetic interactions within these pairs in the micelles and the dynamic properties of both the pairs and separated radicals. Nevertheless, only a few rates of radical exit out of the micellar aggregates and radical recombination therein have been reported so far.[3]

We report here on the application of time-resolved electron-spin-echo (ESE) spectroscopy to study photoreactions in micelles. When this pulsed EPR technique was used to study the primary light reactions in green plant photosystems, an unexpected time-dependent electron echo phase shift (X signal) was observed.[6] It was proposed that this was the result of radical-pair interactions, present at the time of the probing $\pi/2$ microwave pulse, which subsequently decay via radical-pair separation (in contrast to routes that give diamagnetic products) with a lifetime shorter than the experimental time, 2τ (τ is the interval between the $\pi/2$ and π microwave pulses).[6,7] The decay of the X signal thus gives the rate of the radical-pair separation, and the Y signal should give information on the nature of the pair interactions. With our instrumentation, radical pairs with lifetimes of about 0.1–1 μs may exhibit an echo phase shift. Radical pairs in micelles have lifetimes of this order. Therefore, we have undertaken these studies first as a means to verify the mechanism described for the echo phase shift and second to examine the nature and dynamics of radical–radical interactions in micelles.

For our initial ESE investigation, we chose the photoreduction of benzophenone (BP) by 1,4-cyclohexadiene (RH) in sodium dodecylsulfate (SDS) micelles. Scaiano et al. studied this system using transient spectrophotometric-laser photolysis techniques.[3] The scheme shown in eq 1–4 was considered, where the brackets

$$Ph_2CO \xrightarrow{h\nu} {}^1Ph_2CO^* \xrightarrow{ISC} {}^3Ph_2CO^* \quad (1)$$

$${}^3Ph_2CO^* + RH \rightarrow {}^3[Ph_2\dot{C}OH\ \dot{R}] \quad (2)$$

$${}^3[Ph_2\dot{C}OH\ \dot{R}] \xrightarrow{k_{ISC}} {}^1[Ph_2\dot{C}OH\ \dot{R}] \rightarrow \text{products} \quad (3)$$

$${}^3[Ph_2\dot{C}OH\ \dot{R}] \xrightarrow{k_{ESC}} Ph_2\dot{C}OH + \dot{R} \quad (4)$$

represent interacting radical pairs with their respective total spin multiplicities. Assuming that the only fate of the triplet radical pair is either intersystem crossing (reaction 3) or escape from the micelle (reaction 4), the values $k_{ISC} = 5.8 \times 10^6$ s^{-1} and $k_{ESC} = 4.4 \times 10^6$ s^{-1} were determined. It was also noted that it is primarily the cyclohexadienyl radical that exits the micelle. If the reaction is carried out in a magnetic field of 2000 G or greater, the fraction of escaping radicals is 73% in contrast to 43% with no applied field.

The time-resolved ESE experiment has been previously described.[8,9] A Molectron UV 24 nitrogen laser was employed for excitation. Solutions were deaerated by bubbling argon in a reservoir solution that was circulated through a flat cell in the spectrometer cavity.

Figure 1 shows the EPR spectra obtained from the system of BP and 1,4-cyclohexadiene in SDS. Parts a and c of Figure 1 were taken without laser excitation. The "dark" Y signal is that from electron irradiation of the quartz cell and "calibrates" the phase angle. As expected there is no X signal. The spectra taken within 40 ns of laser excitation show a relatively large X signal that has line width and g factor of the BP ketyl radical. To prove that the X signal is a property of the micellar system, Figure 2 shows spectra from BP and 1,4-cyclohexadiene in benzene. The dark signals are the same as in Figure 1, but with laser excitation, only a Y signal of BP ketyl radical is observed. In both solvents, the cyclohexadienyl radical is not observed.

If the observation of the X signal (Figure 1d) is indeed due to radical-pair decay via reaction 4, its kinetic trace should give the escape rate. Figure 3b shows this trace taken at the field value of maximum intensity (Figure 1d). The signal rise is instrument

(5) Lougnot, D.-J.; Jacques, P.; Fonassier, J.-P. *J. Photochem.* **1982**, *19*, 59.
(6) Thurnauer, M. C.; Norris, J. R. *Chem. Phys. Lett.* **1980**, *76*, 557.
(7) Thurnauer, M. C.; Rutherford, A. W.; Norris, J. R. *Biochem. Biophys. Acta* **1982**, *682*, 332.
(8) Trifunac, A. D.; Norris, J. R. *Chem. Phys. Lett.* **1978**, *59*, 140.
(9) Norris, J. R.; Thurnauer, M. C.; Bowman, M. C. *Adv. Biol. Med. Phys.* **1980**, *17*, 365.

limited while its decay lifetime is ~230 ns, in good agreement with the value reported by Scaiano and Abuin.[3]

Detection along Y should give initially a signal due to the interacting pair, which decays via reactions 3 and 4 and subsequently the "growing in" of the free radicals formed via 4. Figure 3a shows the Y kinetic trace. Within experimental error, the Y rise time matches the decay of the X signal. This is expected since k_{ISC} and k_{ESC} are of similar magnitude, while reaction 4 is the main radical-pair decay route in our field of ~3500 G.

According to the above interpretation, the decay rate of the X signal is completely uncoupled from the intersystem crossing rate since the only radical pairs that contribute to the X signal are those that exist as pairs when the first $\pi/2$ microwave signal is applied but have produced a free radical at the time that the echo is observed. In the framework of this model, therefore, $k^X_{obsd} = k_{ESC}$ while $k^Y_{obsd} = k_{ESC} + k_{ISC}$.

Although the signal to noise ratio for the Y signal shown in Figure 1b is rather poor, it is reproducible and can be interpreted as being due to a spin-polarized triplet radical pair with zero field splitting parameters $D \simeq 0.001$ cm^{-1}, $E = 0$ cm^{-1}, giving by the point dipole approximation an average distance between the radicals of ~14 Å.[10] The polarization pattern (emission, enhanced absorption) is that expected for population of the pair from the spin-polarized ^{3}BP[11] and decay from the T_0 level of the radical pair. EPR spectra (Y signal) taken at longer delay times with respect to the laser (not shown) show the BP ketyl radical completely in emission.

In conclusion, this application of time-resolved ESE to photoreactions in micelles supports the mechanism proposed to explain a time-dependent echo phase shift. It also demonstrates that these methods can be used to obtain directly the rate of radical escape from micelles and observe directly radical-pair interactions within the micelle.

Acknowledgment. Fruitful discussion with Drs. A. Trifunac, J. Norris, and R. Lawler are gratefully acknowledged.

Registry No. Benzophenone, 119-61-9; 1,4-cyclohexadiene, 628-41-1; sodium dodecylsulfate, 151-21-3.

(10) Hirota, N.; Weissman, S. I. *J. Am. Chem. Soc.* **1964**, *86*, 2538.
(11) Murai, H.; Imamura, T.; Obi, K. *Chem. Phys. Lett.* **1982**, *87* 295.

^{13}C NMR Evidence of Carbinolamine Formation at the Active Site of an Imine-Forming Aldolase[1]

Bruce David Ray[2] and Edwin T. Harper*

Department of Biochemistry
Indiana University School of Medicine
Indianapolis, Indiana 46223

Wilmer K. Fife

Department of Chemistry
Indiana University—Purdue University at Indianapolis
Indianapolis, Indiana 46223

Received January 20, 1983

In a number of biochemical reactions, carbon–hydrogen and carbon–carbon bonds are activated toward cleavage by conversion of adjacent carbonyl groups to protonated imines, which often can be detected by reductive trapping in the presence of sodium borohydride. The aldol cleavage of ketose phosphates by mammalian fructose 1,6-bisphosphate aldolase (EC 4.2.1.13) is a case in point.[3] Since carbinolamines invariably occur as intermediates in nonenzymic interconversions between carbonyl compounds and imines,[4] it may be reasonable to expect that imine-forming enzymes will also form hitherto undocumented enzyme–substrate carbinolamine intermediates. We now report that the predominant form of the aldolase–glycolaldehyde phosphate complex is an enzyme-stabilized carbinolamine.

Isotopically enriched (90% ^{13}C) D,L[2-^{13}C]glyceraldehyde was synthesized by adaptations of the methods of Serianni et al.,[5] and was converted to [1-^{13}C]glycolaldehyde phosphate (**1**) and [1-^{2}H,1-^{13}C]glycolaldehyde phosphate (**2**) by methods that will be described elsewhere.[6,7] Aldolase was purified from rabbit muscle by the method of Penhoet et al.[8] to a specific activity of 15 units/mg. For spectroscopic studies, aldolase preparations were freed of triose phosphate isomerase activity by treatment with glycidol phosphate[9] and concentrated to 120 mg/mL by precipitation with ammonium sulfate, dialysis, and ultrafiltration. Heavy-metal ions were removed on Chelex-100 (Bio-Rad Laboratories). Spectra were obtained at 8 °C on Nicolet NT-150 or NT-200 NMR (nuclear magnetic resonance) spectrometers operating in the FT mode with quadrature detection over spectral widths of 4500 or 5500 Hz, respectively. Proton decoupling was achieved by 10-W irradiation, during data acquisition only (370 ms/pulse), at 150.0577 or 200.067 15 MHz, respectively. A standard single-pulse sequence was used, with a 1-s delay between pulses and a flip angle of 37°. Chemical shifts were calculated relative to that of an internal standard (dioxane, 67.4 ppm).

The ^{1}H-decoupled ^{13}C NMR spectrum of **1** showed a doublet at 89.9 ppm ($^3J_{CP} = 7.9$ Hz), which was assigned to the $CH(OH)_2$ group of the aldehyde hydrate. No signals were detected in the region near 200–210 ppm, indicating that the aldehyde was at least 97% hydrated. The ^{13}C NMR spectrum of **2**, measured without proton decoupling, consisted of a triplet (89.5 ppm, $^1J_{CD} = 21.8$ Hz) as well as a doublet (90.2 ppm, $^1J_{CH} = 153.8$ Hz), each peak of which represented a poorly resolved doublet arising from ^{13}C–^{31}P coupling. The relative areas of the triplet and the doublet indicated that **2** was 75% deuterated at the aldehyde carbon.

The structure of the aldolase–**2** complex was indicated by the spectrum shown in Figure 1A, compared to that of the enzyme alone (Figure 1B). The striking observation was that the single resonance unique to the complex appeared at 79.7 ppm (shaded peak in Figure 1A), in a region characteristic of sp^3- rather than sp^2-hybridized carbon. The resonance was shown to arise from bound **2** by reappearance[10] of the doublet resonance of free **2** upon displacement by excess (26 mM) hexitol 1,6-bisphosphate.[11] The relative areas (0.06) of the peaks at 79.5 (residual bound **2**) and 87.1 ppm (free **2**)[10] permitted calculation of a dissociation constant (1.3 μM) of the aldolase–**2** complex that is consistent with that (2.5 μM) of the unlabeled complex.[12]

The chemical shift of the new resonance showed that **2** was predominantly bound either as a noncovalent complex of the aldehyde hydrate or as a covalent carbinolamine intermediate, but not as an imine.[13] The complex was identified as a carbi-

(1) Reported in part at the 66th Annual Meeting of the Federation of American Societies for Experimental Biology, New Orleans, LA, Apr 1982.
(2) Present Address: Department of Physics, Indiana University—Purdue University at Indianapolis, IN 46223.
(3) For a review see: Horecker, B. L.; Tsolas, O.; Lai, C. Y. In "The Enzymes", 3rd ed.; Boyer, P. D., Ed.; Academic Press: New York. 1972; Vol. VII, pp 213–258.
(4) Jencks, W. P. *Prog. Phys. Org. Chem.* **1964**, *2*, 63–128; "Catalysis in Chemistry and Enzymology"; McGraw-Hill: New York, 1969; pp 463–554.
(5) Serianni, A. S.; Nunez, H. A.; Barker, R. *Carbohydr. Res.* **1979**, *72*, 71–78. Serianni, A. S.; Clark, E. L.; Barker, R. *Ibid.* **1979**, *72*, 79–91. Serianni, A. S.; Pierce, J., Barker, R. *Biochemistry* **1979**, *18*, 1192–1199. Serianni, A. S.; Barker, R. *Can. J. Chem.* **1979**, *57*, 3160–3167. Serianni, A. S.; Nunez, H. A.; Barker, R. *J. Org. Chem.* **1980**, *45*, 3329–3341.
(6) Ray, B. D. Ph.D. Thesis, Indiana University, Indianapolis, IN, 1982.
(7) The compounds were characterized by thin-layer chromatography, migrating with authentic glycolaldehyde phosphate (R_f 0.43) on cellulose plates in a butanol–water–picric acid solvent. See: Hanes, C. S.; Isherwood, F. A. *Nature (London)* **1949**, *164*, 1107–1112.
(8) Penhoet, E. E.; Kochman, M.; Rutter, W. J. *Biochemistry* **1969**, *8*, 4391–4395.
(9) Rose, I. A.; O'Connell, E. L. *J. Biol. Chem.* **1969**, *244*, 6548–6557.
(10) The resonance reappeared at 87.1 ppm, perhaps due to fast exchange between free and nonspecifically bound forms.
(11) Prepared by the following procedure: Ginsburg, A.; Mehler, A. H. *Biochemistry* **1966**, *5*, 2623–2634.
(12) Rose, I. A.; O'Connell, E. L. *J. Biol. Chem.* **1969**, *244*, 126–134.

0002-7863/83/1505-3731$01.50/0